

# (Z)-2-(2-Bromophenyl)-3-[[4-(1-methyl-piperazine)amino]phenyl]-acrylonitrile (DG172): An Orally Bioavailable PPAR $\beta/\delta$ -Selective Ligand with Inverse Agonistic Properties

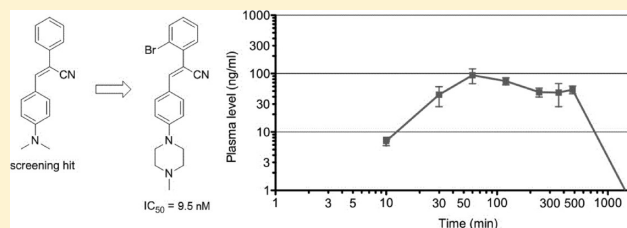
Sonja Lieber,<sup>†,§</sup> Frithjof Scheer,<sup>‡,§</sup> Wolfgang Meissner,<sup>†</sup> Simone Naruhn,<sup>†</sup> Till Adhikary,<sup>†</sup> Sabine Müller-Brüsselbach,<sup>†</sup> Wibke E. Diederich,<sup>\*,‡</sup> and Rolf Müller<sup>\*,†</sup>

<sup>†</sup>Institute of Molecular Biology and Tumor Research (IMT), Philipps University, Emil-Mannkopff-Strasse 2, 35033 Marburg, Germany

<sup>‡</sup>Institute of Pharmaceutical Chemistry, Philipps-University, Marbacher Weg 6, 35032 Marburg, Germany

## Supporting Information

**ABSTRACT:** The ligand-regulated nuclear receptor peroxisome proliferator-activated receptor  $\beta/\delta$  (PPAR $\beta/\delta$ ) is a potential pharmacological target due to its role in disease-related biological processes. We used TR-FRET-based competitive ligand binding and coregulator interaction assays to screen 2693 compounds of the Open Chemical Repository of the NCI/NIH Developmental Therapeutics Program for inhibitory PPAR $\beta/\delta$  ligands. One compound, (Z)-3-(4-dimethylamino-phenyl)-2-phenyl-acrylonitrile, was used for a systematic SAR study. This led to the design of derivative 37, (Z)-2-(2-bromophenyl)-3-[[4-(1-methyl-piperazine)amino]phenyl]acrylonitrile (DG172), a novel PPAR $\beta/\delta$ -selective ligand showing high binding affinity ( $IC_{50} = 27$  nM) and potent inverse agonistic properties. 37 selectively inhibited the agonist-induced activity of PPAR $\beta/\delta$ , enhanced transcriptional corepressor recruitment, and down-regulated transcription of the PPAR $\beta/\delta$  target gene *Angptl4* in mouse myoblasts ( $IC_{50} = 9.5$  nM). Importantly, 37 was bioavailable after oral application to mice with peak plasma levels in the concentration range of its maximal inhibitory potency, suggesting that 37 will be an invaluable tool to elucidate the functions and therapeutic potential of PPAR $\beta/\delta$ .



## INTRODUCTION

Members of the class II subset of nuclear receptors, including the thyroid hormone receptor, the retinoic acid receptor, and peroxisome proliferator-activated receptors (PPARs), can actively repress target genes in the absence of ligand binding but activate the same genes if bound by an agonistic ligand.<sup>1</sup> These activities are linked to the induction of distinct local chromatin structures depending on the presence or absence of an agonistic ligand. The three PPAR subtypes (PPAR $\alpha$ , PPAR $\beta/\delta$ , and PPAR $\gamma$ ) regulate their target genes through binding to specific DNA elements (PPREs) as obligatory heterodimers with the retinoid X receptor. Certain lipids, fatty acid metabolites, and subtype-selective synthetic ligands modulate their transcriptional activity,<sup>2-4</sup> suggesting that PPARs act as sensors for both endogenous and exogenous stimuli, which impinge not only on intermediary metabolism but also on inflammatory pathways.<sup>5</sup> In addition to these functions, PPARs figure in development, wound healing, cell differentiation, proliferation, and apoptosis.<sup>6-8</sup>

PPRE-bound PPAR $\beta/\delta$  complexes have functions in both transcriptional repression and transcriptional activation. Agonistic ligands induce a conformational change in PPARs that favors the association with coactivators and the dissociation of corepressors.<sup>9</sup> Many PPAR-interacting coregulators have been described, including histone acetyl transferases (HATs) and HAT-recruiting coregulators, histone deacetylases (HDACs)

and HDAC recruiting factors, protein arginine methyl transferases, and factors with chromatin remodeling functions. While the role of histone acetylation in PPAR-mediated transcriptional activation is well established, the exact role of other enzymatic modifications and coregulators remains unclear, in particular for the PPAR $\beta/\delta$  subtype. The mechanisms of PPAR $\beta/\delta$ -mediated repression by PPRE-bound unliganded receptors are even less understood. A number of corepressors have been identified, such as class I HDACs, NCoR/SMRT, and SHARP,<sup>10</sup> but their precise function in the regulation of specific target genes involving the ordered assembly and disassembly of multiprotein complexes is not known. The complexity of PPAR $\beta/\delta$ -mediated transcriptional regulation is further complicated by the fact that distinct regulatory mechanisms govern the expression of different sets of target genes.<sup>11</sup> Thus, repression appears to represent the major mode of PPAR $\beta/\delta$ -mediated transcriptional regulation, and only a subset of target genes is subject to an agonist-mediated switch from active repression to activation. Finally, PPARs can also regulate genes without making direct DNA contacts by directly interacting with specific transcription factors, as exemplified by the repression of BCL-6 by PPAR $\beta/\delta$ .<sup>12</sup>

Received: January 2, 2012

Published: February 27, 2012

Because of these complexities, the correlation of biological functions and transcriptional pathways regulated by PPAR $\beta/\delta$  is difficult. This is exemplified by the genetic disruption of *Ppard* genes, which can have opposite effects of individual PPAR $\beta/\delta$  target genes, depending on their mode of transcriptional regulation, which in turn hampers the assessment of PPAR $\beta/\delta$  as a potential target for pharmacological inhibition. While potent synthetic agonists that are bioavailable, selective for PPAR $\beta/\delta$ , and bind reversibly are available, inhibitory ligands for PPAR $\beta/\delta$  fulfilling these criteria have not been described to date. Both 2-(2-methyl-4-((4-methyl-2-(naphthalen-1-yl)thiazol-5-yl)methylthio)phenoxy)acetic acid (SR13904)<sup>13</sup> and 4-chloro-*N*-(2-((5-trifluoromethyl-2-pyridyl)sulfonyl)ethyl)benzamide (GSK3787)<sup>14,15</sup> are not specific for PPAR $\beta/\delta$ , and GSK3787 binds PPAR $\beta/\delta$  irreversibly, which is pharmacologically undesirable. 3-(((2-Methoxy-4-(phenylamino)phenyl)amino)sulfonyl)-2-thiophenecarboxylate (GSK0660)<sup>16</sup> is PPAR $\beta/\delta$  subtype-specific but is not bioavailable. This also applies to methyl 3-(*N*-(4-(hexylamino)-2-methoxyphenyl)sulfamoyl)thiophene-2-carboxylate (ST247), a recently developed GSK0660 derivative with greatly improved affinity.<sup>17,18</sup> These ligands are not only competitive antagonists but exert their inhibitory function as inverse agonists, as indicated by their inhibitory effect on the basal expression of PPAR $\beta/\delta$  target genes and an increased recruitment of transcriptional corepressors.<sup>15–17</sup> Finally, a biphenylcarboxylic acid-based antagonist has been described, but its *in vivo* performance has not been addressed.<sup>19</sup>

In light of the lack of inhibitory PPAR $\beta/\delta$  ligands suitable for *in vivo* applications, we have searched for novel chemical structures that could serve as leads for the development of improved inverse agonists. Toward this end, we screened a chemical compound library and identified several stilbene-based or -related inhibitory PPAR $\beta/\delta$  ligands. One of these compounds was chosen for further development and the establishment of structure–activity relationships. This finally yielded a compound with the desired properties, including high affinity, specificity, and bioavailability after oral application.

## RESULTS AND DISCUSSION

**Screening for Inhibitory PPAR $\beta/\delta$  Ligands.** A TR-FRET-based competitive ligand-binding assay was used to screen 2693 compounds of the Open Chemical Repository of the NCI/NIH Developmental Therapeutics Program for PPAR $\beta/\delta$  ligands. In this assay, the terbium-labeled PPAR $\beta/\delta$  LBD interacts with the fluorescent PPAR ligand Fluormone Pan-PPAR Green, which produces FRET from terbium (495 nm) to Pan-PPAR Green (520 nm). Displacement of the fluorescent ligand by an unlabeled test compound results in a quantifiable attenuation of FRET. Out of 191 identified compounds, 10 disrupted the interaction of the PPAR $\beta/\delta$  LBD with a coactivator peptide in a TR-FRET-based assay (Supporting Information Table S1). Four of these compounds possess a stilbene-based or -related core structure. In this assay, interaction of the PPAR $\beta/\delta$  LBD (indirectly labeled by terbium) with the fluorescein-labeled coactivator peptide C33 is determined. The data therefore indicates that these 10 compounds act as inhibitory ligands. Eight of these ligands were also able to trigger the association with the SMRT-ID2 peptide, derived from the interaction domain 2 of the corepressor SMRT, which qualifies these compounds as inverse agonists. Two of these ligands, NSC667251 and compound **1** (NSC636948), also showed efficacy in cell-based assays, i.e., repression of agonist-induced transcription in a luciferase reporter assay and repression of the endogenous PPAR $\beta/\delta$  target

gene ANGPTL4 (Supporting Information Table S1). Compound **1**, which is (Z)-3-[4-(dimethylamino)phenyl]-2-phenylacrylonitrile, was used as a lead structure for further development, as described in detail below.

Among the eight compounds identified as inverse agonists is the clinically important drug (Z)-2-[4-(1,2-diphenylbut-1-enyl)-phenoxy]-*N,N*-dimethylethanamine (tamoxifen) (Supporting Information Table S1). However, in spite of efficient corepressor recruitment *in vitro*, no activity was detectable in the cell-based assays. The same observations were made with three metabolites of tamoxifen, i.e., 4-OH-tamoxifen, *N*-desmethyl-tamoxifen, and endoxifen (Supporting Information Table S2). Because these compounds are able to modulate estrogen receptor-driven gene expression in intact cells, their failure to affect PPAR $\beta/\delta$  activity cannot be attributed to a lack of cellular uptake. It is possible that the subcellular compartmentalization of tamoxifen and its metabolites is a limiting step restricting the accessibility of target proteins. We also analyzed other commercially available stilbenes, including the pharmacologically relevant compounds resveratrol and diethylstilbestrol, but did not observe any significant activities (Supporting Information Table S2). These observations show that binding to PPAR $\beta/\delta$  is not a general property of stilbenes.

**Optimization of the Screening Hit 1.** **1** was chosen as starting point for optimization (Figure 1). We first turned our

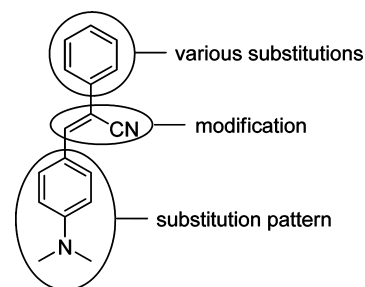


**Figure 1.** Strategy for optimization of the initial screening hit **1**.

attention toward the central acrylonitrile moiety. However, modification at this position, e.g., by hydrogenation **2**, removal **3** or alteration of the position of the nitrile functionality **4**, or elongation leading to the 1,3-butadiensystem **5** resulted in a complete loss of activity (Supporting Information Figure S1). Therefore, the acrylonitrile moiety seems to be crucial for activity. We then examined the effect of the *para*-dimethylamino-substituent present in **1**. Removal (**6**) or replacement by a variety of either electron-withdrawing or electron-donating functional groups (**7–12**) again led to a significant drop in affinity. The only exception turned out to be **13** bearing a primary amino functionality in *para*-position, indicating that the existence of an electron-related push–pull system is essential for activity (Supporting Information Figure S1). Consequently, introduction of a dimethylaminomethylene substituent in *para*-position **14** (Figure 2) and thus disruption of the conjugated push–pull system also diminished the binding affinity toward the PPAR $\beta/\delta$ -LDB significantly. Because the *para*-dimethylamino derivative **1** possessed a higher binding affinity than the unsubstituted *para*-amino-representative **13**, we focused our attention on the substitution pattern of this essential amino group to achieve a further increase in binding affinity (Figure 2). Besides tertiary amines of varying ring sizes, such as in pyrrolidine- (**15**),

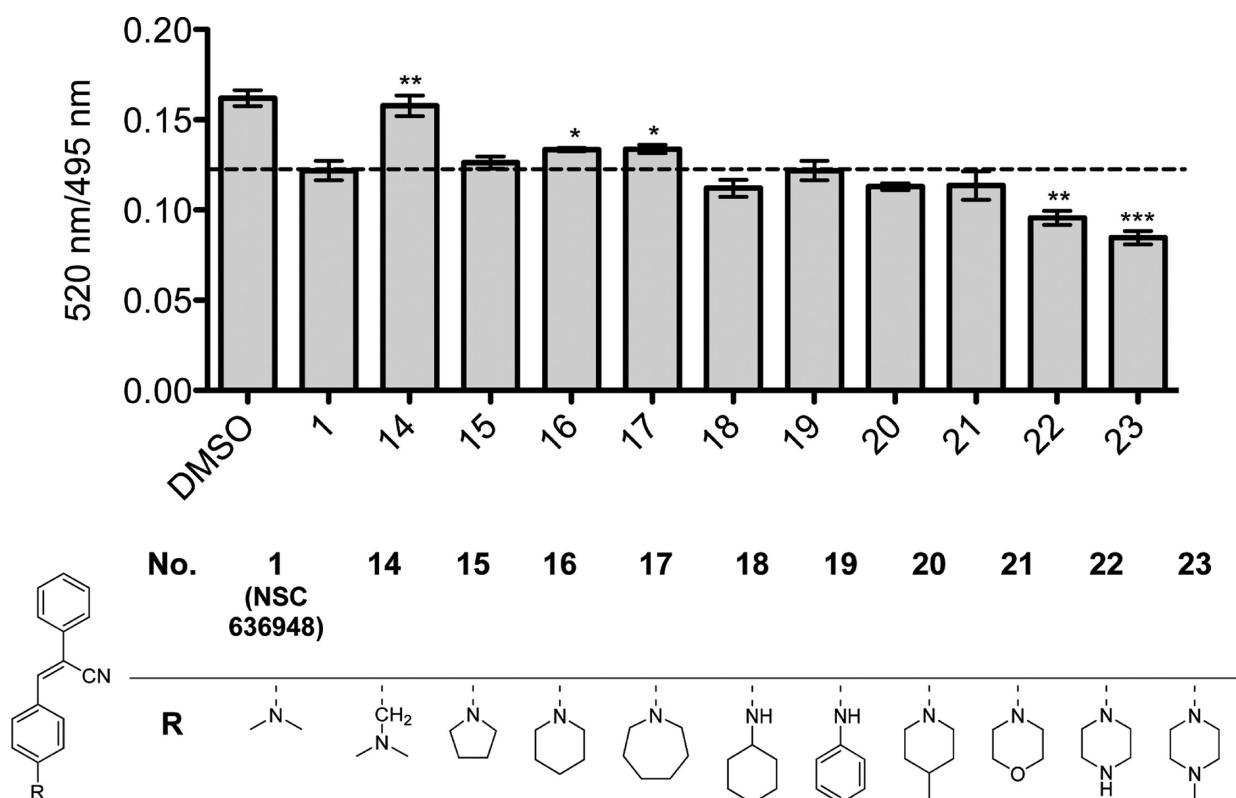


**Figure 2.** Activity of **1** and the indicated derivatives as PPAR $\beta/\delta$  ligands determined in vitro by competitive ligand binding assay. Displacement of a fluorescent PPAR ligand (Fluormone Pan-PPAR Green) from recombinant GST-PPAR $\beta/\delta$  by the indicated compounds was determined by TR-FRET. Each compound was tested at a concentration of 1  $\mu$ M. Results are expressed as the ratio of fluorescence intensity at 520 nm (fluorescein emission excited by terbium emission) and 495 nm (terbium emission). All data points represent averages of triplicates ( $\pm$ SD). \*\*\*, \*\*, and \*: significant difference to compound **1** by *t* test ( $P < 0.001$ ,  $P < 0.01$ , and  $P < 0.05$ , respectively).

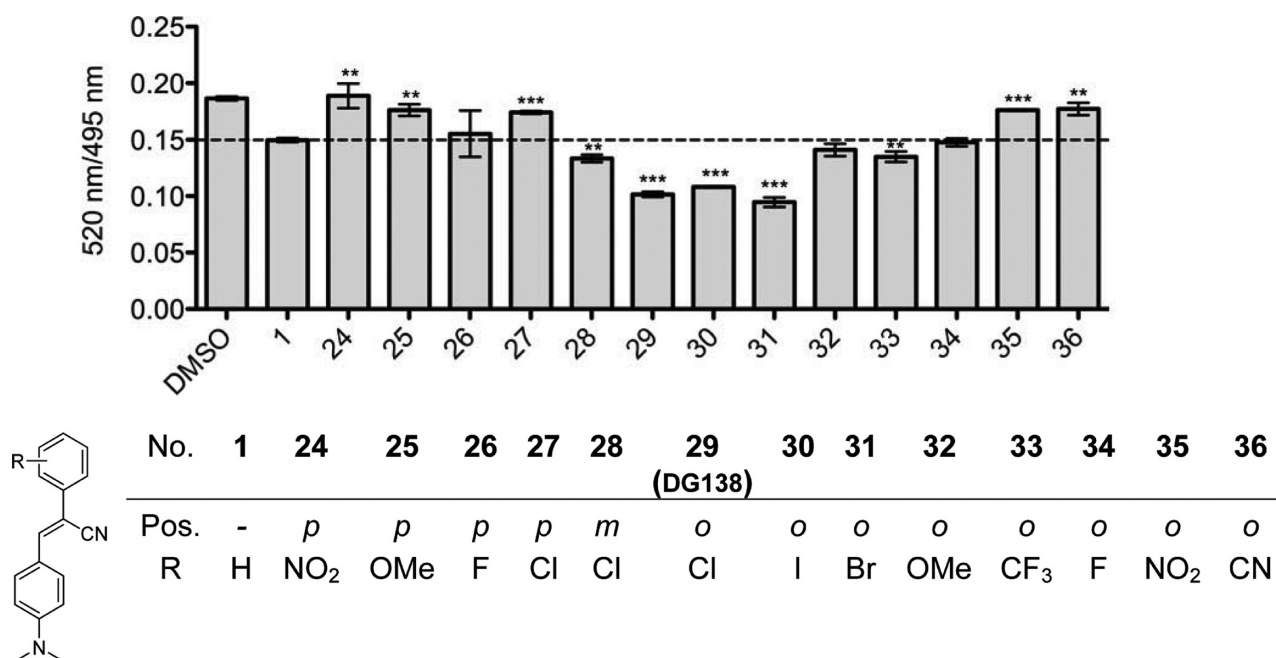


**Figure 3.** Activity of compound **1** and the indicated derivatives as PPAR $\beta/\delta$  ligands. All experimental details were as in Figure 2.

piperidine- (**16**), or azepane- (**17**) substituted structures present, we also tested two secondary amines (**18**, **19**).

Although the competitive TR-FRET assay showed only slight differences between these compounds, the piperidine analogue gave the best results in a cell-based luciferase reporter assay

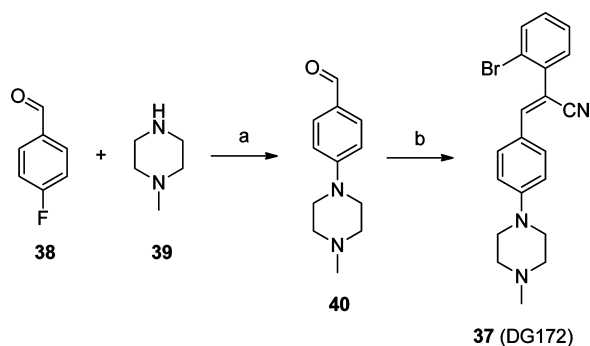
(data not shown). Hence, further compounds bearing six-membered heterocycles were synthesized. Introduction of a 4-methylpiperidino (**20**), a morpholino (**21**), and a piperazine (**22**) moiety, respectively, led to a significant gain in affinity. The best compound within this series was found to be **23**

equipped with a 4-methylpiperazino substituent. The two secondary amines, the aniline- (19) as well as the cyclohexylamine-derivative (18), also possessed a higher binding affinity compared to 1 but could still not compete with 23.

We then turned our attention to the second aromatic portion within this compound class (Figure 3). The initial screening hit 1 was likewise used as reference. However, any tested substituent introduced in *para*-position of this phenyl substituent led to a decrease in binding affinity, indicating that there might only be limited space available within the respective binding pocket (24–27). On the contrary, introducing a chlorine substituent in *meta*-position 28 gave a significant improvement in binding affinity. This effect was even more pronounced for this substituent in *ortho*-position as in compound 29 (DG138). Iodine as *ortho*-substituent 30 performed equally well while compound 31, equipped with a bromine in this position, turned out to be the most potent ligand within this series. Introduction of other substituents with a stronger -I-effect such as 32, 33, and 34 only led to a slight increase in comparison to 1 or even resulted in a decrease in binding affinity when strong electron withdrawing groups (35, 36) were introduced.

Combination of the substitution patterns of the most active compounds of both series, i.e., halogenation in the *ortho*-position and the introduction of a 4-methylpiperazine, finally led to derivative 37 (DG172) (see Scheme 1), analyzed in detail below.

Scheme 1. Synthesis of 37<sup>a</sup>



<sup>a</sup>Reagents and conditions: (a)  $K_2CO_3$ , DMSO, 100 °C, 78% (b) 2-bromophenylacetonitrile, pyrrolidine, MeOH, 60 °C, 79%.

The compounds described above are easily accessible via a Knoevenagel condensation, which exclusively yield the (*Z*)-isomers (for example,  $^3J_{(H,C)} = 14.4$  Hz for 1), employing the corresponding aldehydes and phenylacetonitriles under basic conditions. For the preparation of several of the amino-derivatives, 4-bromophenylaldehyde was employed in the Knoevenagel reaction, followed by a Buchwald–Hartwig reaction<sup>20–22</sup> to introduce the respective amino substituent. In case of 37, 4-fluorobenzaldehyde 38 was first reacted with 4-methylpiperazine 39 to 40, followed by a Knoevenagel condensation employing 2-bromophenylacetonitrile, as outlined in Scheme 1.

**Binding Affinities and Inhibitory Properties of 29 and 37 in vitro.** We next analyzed 37 in further detail with respect to its binding affinity, inhibitory properties, and specificity. First, 37 was compared to both 29 (harboring the *ortho*-halogenation but lacking the 4-methylpiperazine) and its parent molecule 1 in a competitive ligand binding assay. The data in Figure 4A shows that 29 possesses a significantly enhanced affinity compared to 1 and performed similarly as a published reference compound, GSK0660. As expected, 37 was the most potent compound with

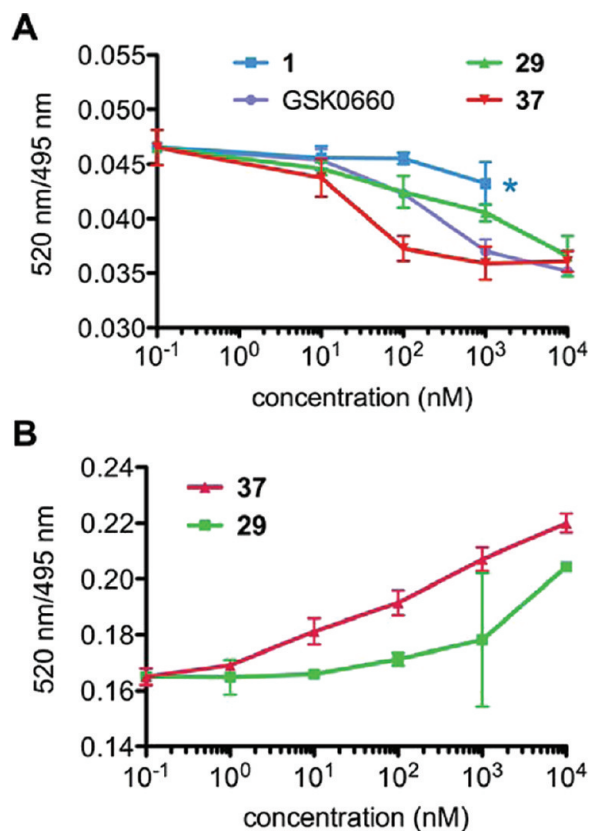


**Figure 4.** In vitro binding and interaction properties of compound 1 and its derivatives 29 and 37. (A) FRET-based competitive ligand binding assay as in Figure 2. GSK0660 is included for comparison. \*Measurement of 1 at 10  $\mu$ M was not possible due to a lack of solubility. (B) Comparison of 29- and 37-induced binding of a corepressor-derived peptide to the PPAR $\beta/\delta$  LBD. Interaction of SMRT-ID2 peptide (fluorescein labeled) and recombinant GST-PPAR $\beta/\delta$  (labeled by a terbium-coupled anti-GST antibody) was measured by TR-FRET. In both panels, results are expressed as the ratio of fluorescence intensity at 520 nm (fluorescein emission excited by terbium emission) and 495 nm (terbium emission). All data points represent averages of triplicates ( $\pm$ SD). \*\*\*, \*\*, and \*: significant difference by *t* test compared to untreated sample ( $P < 0.001$ ,  $P < 0.01$ , and  $P < 0.05$ , respectively).

an  $IC_{50}$  value of 26.9 nM, compared to  $\sim$ 180 nM for 29 and  $>$ 300 nM for GSK0660 (values are averages from three independent experiments each analyzing five different concentrations as triplicates). The latter two values cannot be accurately determined due to a lack of solubility at high concentrations.

To evaluate the inhibitory properties of 29 and 37, we investigated the effect of these compounds on the interaction of PPAR $\beta/\delta$  with the synthetic corepressor peptide SMRT-ID2 by TR-FRET. The data obtained by this assay (Figure 4B) show a clearly enhanced interaction for 37 compared to 29 and thus closely mirror the results obtained by the competitive binding assay (Figure 4A). The data also confirm both ligands as inverse agonists.

**Specificity for PPAR $\beta/\delta$ .** The PPAR subtype specificity of 29 and 37 was addressed by a competitive TR-FRET assay. The data in Figure 5 show that at 1  $\mu$ M both compounds selectively competed for binding to PPAR $\beta/\delta$ . Competition for binding to PPAR $\alpha$  or PPAR $\gamma$  was extremely low or undetectable. In contrast, the PPAR $\alpha$  agonist GW7647, the PPAR $\beta/\delta$  agonist GW501516, and the PPAR $\gamma$  agonist GW1929 strongly interacted with the

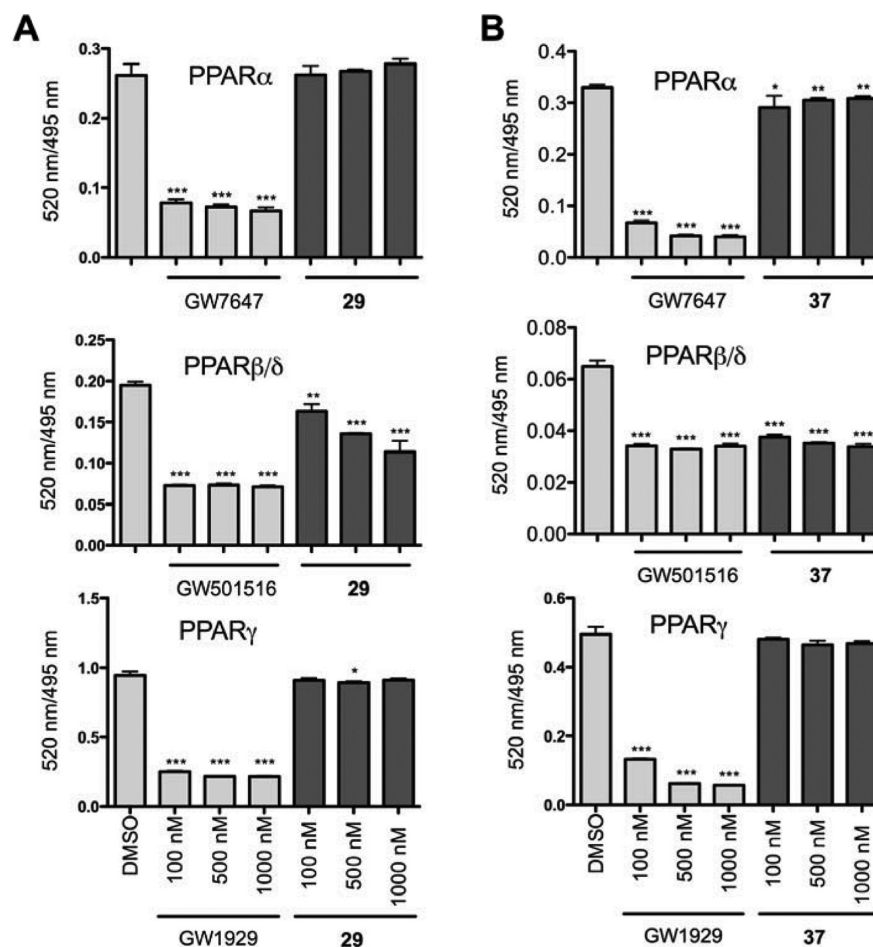


**Figure 5.** PPAR subtype binding specificity. Competition of **29** (A) or **37** (B) with Fluormone Pan-PPAR Green for binding to PPAR $\alpha$ , PPAR $\beta/\delta$ , and PPAR $\gamma$  compared to the PPAR $\alpha$  agonist GW7647 (top), the PPAR $\beta/\delta$  agonist L165,041 (middle), the PPAR $\gamma$  agonist GW1929 (bottom), or solvent (DMSO) only. Experimental details are described in Figure 4.

respective PPAR subtype (Figure 5), thus confirming the validity of the assay.

We next analyzed the effect of both compounds (and of GSK0660 for comparison) on the agonist-induced transcriptional activity of PPAR $\alpha$ , PPAR $\beta/\delta$ , and PPAR $\gamma$  in a cell-based assay. As shown in Figure 6, treatment with subtype-selective agonists resulted in a 3–7.5-fold activation of the respective PPAR subtype in luciferase reporter assays. Whereas **29** and **37** had no significant effect on PPAR $\alpha$ - or PPAR $\gamma$ -driven transcription, they both efficiently antagonized ligand activation of PPAR $\beta/\delta$ , which is consistent with the results of the in vitro ligand-binding assay described above.

**Inhibition of Endogenous PPAR $\beta/\delta$  Target Gene Expression.** The inverse agonistic properties of **29** and **37** were tested in an endogenous cellular context by investigating their effect on the established PPAR $\beta/\delta$  target gene *Angptl4*.<sup>23,24</sup> Toward this end, we performed titration experiments to determine the IC<sub>50</sub> values for **29** and **37** in C2C12 mouse myoblasts (Figure 7A). The parent compound **1** and GSK0660 were included in this study for comparison. This analysis clearly revealed the superior effect of **37** (IC<sub>50</sub> = 9.5 nM) compared to the other compounds, which showed IC<sub>50</sub> values of 52 nM (**29**), >500 nM (**1**), and 48 nM (GSK0660), respectively (values are averages from three independent experiments each analyzing six different concentrations as triplicates). Because the tested compounds had no detectable effect on PPAR $\alpha$  and PPAR $\gamma$  (Figures 5 and 6), it is very likely

that the observed effect on *Angptl4* expression is mediated through PPAR $\beta/\delta$ . This is strongly supported by our observation that the inhibition of *Angptl4* expression by **37** was dependent on the presence of wild-type PPAR $\beta/\delta$  alleles (Figure 7B).

**Effect on Corepressor Recruitment to Chromatin-Bound PPAR $\beta/\delta$ .** To investigate the effect of **37** on the assembly of chromatin-associated corepressor complexes, we performed chromatin immune precipitation (ChIP) analyses of HDAC3 recruitment to the *ANGPTL4* gene in WPMY-1 human myofibroblasts. As can be seen in Figure 8A, **37** induced an enhanced recruitment of HDAC3 compared to solvent-treated cells (DMSO). The specificity of the ChIP assay was shown by the lack of antibody binding to an irrelevant region of the *PDK4* gene (Figure 8B) and by the lack of any detectable effect on HDAC3 binding (Figure 8A) of reference compound **41**, which is a pure PPAR $\beta/\delta$  antagonist and therefore unable to enhance corepressor recruitment.<sup>17</sup> The data in Figure 8A also show that GSK0660 and **37** have similar effects, which do not correlate with the higher potency of **37** to repress *ANGPTL4* transcription (Figure 7A). We attribute this to the possibility that other corepressors are instrumental in **37**-mediated repression, as suggested by the multitude of coregulators interacting with repressive PPAR complexes.

**Pharmacokinetics in Mice.** Finally, to determine the potential suitability of **29** and **37** for in vivo applications, pharmacokinetic studies were carried out in mice. **29** and **37** were administered intravenously (1 mg/kg) and orally (5 mg/kg),

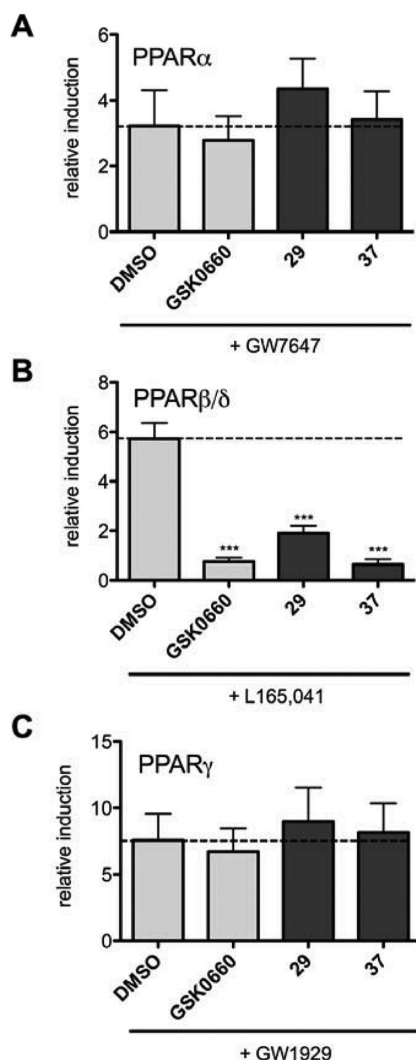


**Figure 6.** Effects on the agonist-induced transcriptional activity of LexA-PPAR $\alpha$  (A), LexA-PPAR $\beta/\delta$  (B), and LexA-PPAR $\gamma$  (C). NIH3T3 cells were transiently transfected with a luciferase reporter plasmid containing multiple LexA binding sites. Four hours post-transfection, the cells were treated with the indicated inhibitory ligands (1  $\mu$ M) for 48 h, followed by 300 nM of the PPAR $\alpha$  agonist GW7647, 1  $\mu$ M of the PPAR $\beta/\delta$  agonist L165,041, or 300 nM of the PPAR $\gamma$  agonist GW1929 or agonist solvent. GSK0660 (1  $\mu$ M) is included for comparison. Induction values represent luciferase activities of agonist-treated cells relative to cells treated with agonist solvent. Statistical analysis was performed as in Figure 4.

blood samples were analyzed 10 min to 12 h post-treatment by HPLC-MS (Figure 9), and basic pharmacokinetic parameters were determined. After intravenous administration of 37, a plasma half-life of 76 min was measured, the mean clearance (CL) was 121 mL/min/kg, and the volume of distribution at steady state (V<sub>ss</sub>) 12.5 L/kg. Oral administration yielded a good exposure with an AUC<sub>inf</sub> of 8239 min·ng/mL and a peak plasma level (C<sub>max</sub>) of 94 ng/mL (207 nM), which is clearly within the concentration range of maximal activity determined in vitro (IC<sub>50</sub> = 23 nM; Figure 4A) or in cell culture (IC<sub>50</sub> = 6.5 nM for C2C12 cells; Figure 7A). Furthermore, half-life (634 min) and bioavailability (72%) were in the desired range. This pharmacokinetic data set suggests that 37 is suitable for in vivo applications in mice, including its peroral administration. In contrast, despite an acceptable plasma half-life after intravenous injection of 76 min

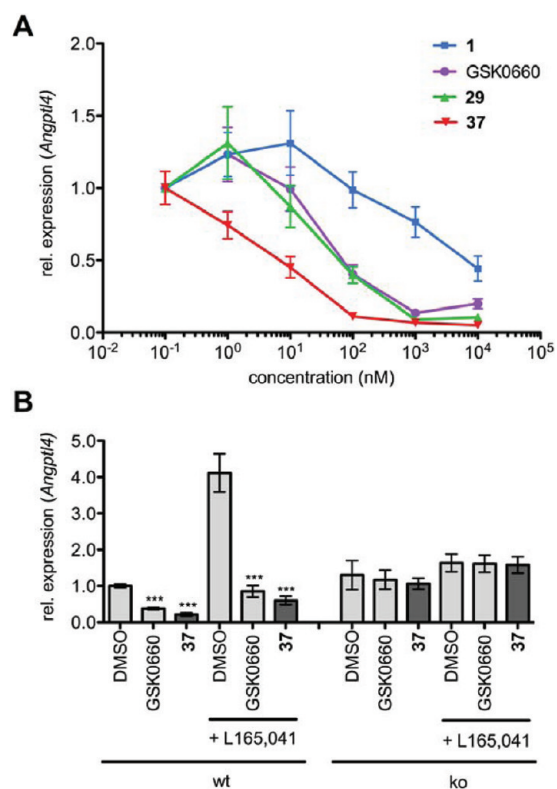


**Figure 7.** Impact on expression of the endogenous PPAR $\beta/\delta$  target gene *Angptl4*. (A) C2C12 mouse myoblasts were treated for 24 h with 1, 29, and 37 at the indicated concentration, and RNA was analyzed by RT-qPCR. GSK0660 is included for comparison. (B) Dependence on PPAR $\beta/\delta$ . Macrophages from *Ppard* wild-type (WT) and null (KO) mice were treated with the agonist L165,041 (500 nM), 37 (1  $\mu$ M), GSK0660 (1  $\mu$ M), or with solvent only (DMSO) for 6 h, and the expression of *Angptl4* was determined by RT-qPCR. Statistical analysis was performed as in Figure 4.

(CL = 176 mL/min/kg; V<sub>ss</sub> = 6.2 L/kg), 29 was detectable in the blood at very low levels ( $\leq 6$  ng/mL) and for a short time following oral application ( $\leq 30$  min), indicating a lack of bioavailability.

## CONCLUSIONS

By screening a chemical compound library, we identified (*Z*)-3-[4-(dimethylamino)phenyl]-2-phenylacrylonitrile (1) as an inhibitory PPAR $\beta/\delta$  ligand. A comprehensive SAR study revealed two modifications, *ortho*-halogenation and introduction of an *N*-4-methylpiperazine moiety, that greatly improved the binding affinity for PPAR $\beta/\delta$  and the efficiency of corepressors. The combination of these two critical modifications led to the discovery of (*Z*)-2-(2-bromophenyl)-3-[[4-(1-methylpiperazine-amino)phenyl]acrylonitrile (37), which is the most potent inverse agonist for PPAR $\beta/\delta$  known to date. 37 is PPAR-subtype selective and inhibits both agonist-induced and basal level PPARE-dependent transcription in cells. Most importantly, 37 has good oral pharmacokinetic properties, making it the first bioavailable PPAR $\beta/\delta$ -selective inverse agonist described to date. 37 therefore represents a useful novel tool to investigate the biological and pathophysiological functions of PPAR $\beta/\delta$  and to clarify its potential as a target for drug development.

## EXPERIMENTAL SECTION

**Ligands.** {2-Methyl-4-[[4-methyl-2-[4-(trifluoromethyl)phenyl]-1,3-thiazol-5-yl]methyl]sulfanyl]phenoxy}acetic acid (GW501516) was

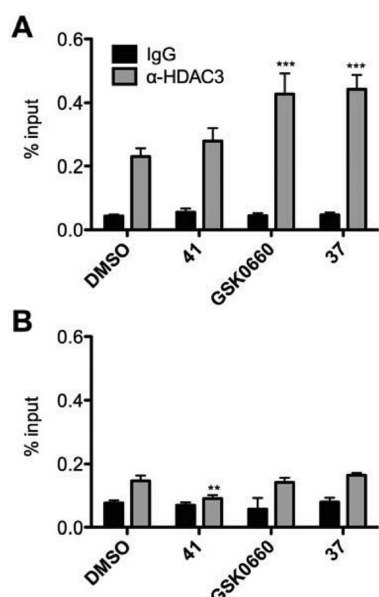


**Figure 8.** Corepressor binding to PPAR $\beta/\delta$ . The impact of 37 on recruitment of HDAC3 to the *ANGPTL4* promoter in WPMY-1 myofibroblasts was determined by ChIP. Compound 41 does not induce corepressor recruitment<sup>17</sup> and was used as a negative control. Cells were treated with the indicated compounds (1  $\mu$ M) for 30 min. ChIP was carried out using antibodies against HDAC3 or a nonspecific rabbit IgG pool (negative control). DNA was amplified with primers encompassing the *ANGPTL4* PPREs (A) or a control region (B). Relative amounts of amplified DNA in immunoprecipitates were calculated by comparison with 1% of input DNA. Results are expressed as % input. Statistical analysis was performed as in Figure 4.

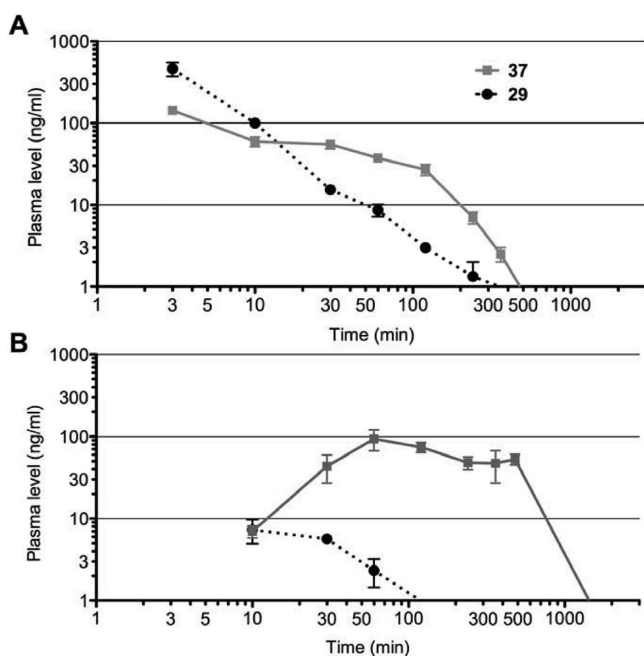


**Figure 9.** Pharmacokinetics in mice. 29 and 37 were administered either intravenously at a dose of 1 mg/kg (A) or orally at 5 mg/kg (B), and blood samples were analyzed by HPLC-MS/MS at the indicated time points post-treatment. Results represent averages of biological triplicates ( $\pm$ SD). Both compounds were undetectable at 24 h.

purchased from Axxora (Lörrach, Germany), *N*-(2-benzoylphenyl)-O-[2-(methyl-2-pyridinylamino)ethyl]-L-tyrosine hydrochloride (GW1929)

and 4-[3-(2-propyl-3-hydroxy-4-acetyl)phenoxy]propoxyphenoxyacetic acid (L165,041) from Biozol (Eching, Germany), and 2-(4-{2-[4-cyclohexylbutyl(cyclohexylcarbamoyl)amino]ethyl}phenyl)sulfanyl-2-methylpropanoic acid (GW7647) from Sigma-Aldrich (Steinheim, Germany). Synthesis of GSK0660 and compound 41, 3-[*N*-[4-(*tert*-butylamino)-2-methoxyphenyl]sulfamoyl]-thiophene-2-carboxylate (PT-SS8), has been reported previously.<sup>19</sup>

**Chemistry.** Reagents and solvents that are commercially available were used without further purification. Thin layer chromatography was performed on precoated plates silica gel 60 F254, Merck. Flash column chromatography was performed on prepacked flash chromatography columns (PF 30-SIHP-JP/12G) purchased from Interchim and using a Büchi separation system. Cyclohexane was purchased in pa quality from Grüssing and distilled prior to use, and *iso*-hexane was purchased in technical quality and distilled prior to use.

<sup>1</sup>H NMR and <sup>13</sup>C NMR spectra were recorded on a Jeol ECX-400 or on a Jeol ECA-500 spectrometer. Chemical shifts ( $\delta$ ) are given in ppm with the residual solvent signal used as reference (CDCl<sub>3</sub>: s, 7.26 ppm [<sup>1</sup>H] and t, 77.1 ppm [<sup>13</sup>C]; DMSO-*d*<sub>6</sub>: quint, 2.50 ppm [<sup>1</sup>H] and septet, 40.1 ppm [<sup>13</sup>C]). Unless otherwise noted, spectra with CDCl<sub>3</sub> as solvent were recorded at 20 °C while spectra with DMSO-*d*<sub>6</sub> as solvent were recorded at 30.0 °C. Peak patterns were described as follows: s (singlet), d (doublet), dd (double doublet), ddd (doublet of doublet of doublet), t (triplet), m (multiplet), sm (symmetric multiplet), bs (broad singlet), psd (pseudo doublet). Mass spectra were recorded on a double-focusing sector field spectrometer type 70-70H (Vacuum Generators) or on a double-focusing sector field spectrometer type AutoSpec (Micromass). Elemental combustion analyses were performed on a Vario MICRO cube (Elementar Analysensysteme GmbH, Hanau, Germany). Melting points were determined using a melting point meter KSPIN (A. Krüss Optronic GmbH, Hamburg, Germany) and are uncorrected.

All tested compounds were at least 95% pure as a single isomer, determined by NMR and combustion analysis.

**Procedure A:** To a solution of the respective phenylacetonitrile (1 equiv) and the corresponding benzaldehyde (1 equiv) in methanol (0.6 M) was added potassium hydroxide, and the reaction mixture was stirred at RT until TLC indicated full conversion of the starting material. The precipitate was collected, washed with water and hexane, and dried in vacuo.

**Procedure B:** To a solution of the respective phenylacetonitrile (1 equiv) and the corresponding benzaldehyde (1 equiv) in methanol (0.6 M) was added pyrrolidine, and the reaction mixture was stirred until TLC indicated full conversion of the starting material. The precipitate was collected, washed with water and hexane, and dried in vacuo.

**Procedure C:** (*Z*)-3-(4-Bromophenyl)-2-phenylacrylonitrile (1 equiv, prepared following procedure A) was dissolved in dry toluene (0.7 M) under argon atmosphere. ( $\pm$ )-BINAP (0.075 equiv), Pd<sub>2</sub>(dba)<sub>3</sub> (0.05 equiv), sodium *tert*-butoxide (1.5 equiv), and the corresponding amine (2 equiv) were added, and the suspension was stirred at 80 °C until thin layer chromatography indicated full conversion of the starting material. The reaction mixture was diluted with DCM, filtered through a pad of Celite, adsorbed on silica gel, and purified by flash chromatography.

(*Z*)-3-[4-[(*Dimethylamino*)methyl]phenyl]-2-phenylacrylonitrile Hydrochloride (14). To a solution of 4-[(*dimethylamino*)methyl]-benzaldehyde (105 mg, 0.90 mmol) and phenylacetonitrile (105 mg, 0.90 mmol) in methanol (2 mL) was added potassium hydroxide (50 mg, 0.90 mmol), and the reaction mixture was stirred for 24 h at RT. The reaction mixture was diluted with EtOAc, and the organic phase was washed with water, saturated potassium hydrogencarbonate solution and brine, dried over MgSO<sub>4</sub>, filtered, and concentrated in vacuo. The free base was obtained by flash chromatography (hexane/EtOAc, gradient from 0 to 50% in 15 min) and was afterward converted to the hydrochloride salt 14 (120 mg, 0.40 mmol, 45%) by precipitation from EtOAc with HCl (5–6 M in *i*-PrOH); mp above decomposition temperature. <sup>1</sup>H NMR (DMSO-*d*<sub>6</sub>)  $\delta$  11.04 (bs, 1H), 8.07 (s, 1H), 7.97 (psd, *J* = 8.2 Hz, 2H), 7.78–7.71 (m, 4H), 7.54–7.48 (m, 2H), 7.47–7.42 (sm, 1H), 4.31 (s, 2H), 2.68 (s, 6H). <sup>13</sup>C NMR (DMSO-*d*<sub>6</sub>)  $\delta$  142.6, 135.2, 134.1, 133.3, 132.1, 130.1, 129.9, 129.8, 126.4, 118.3, 111.9, 59.4, 42.1. HRMS (EI) calcd for C<sub>18</sub>H<sub>18</sub>N<sub>2</sub>

[M]<sup>+</sup> 262.146999; found 262.145737. Anal. Calcd for C<sub>18</sub>H<sub>19</sub>ClN<sub>2</sub>: C, 72.35; H, 6.41; N, 9.37. Found: C, 71.83; H, 6.52; N, 9.21.

(Z)-2-Phenyl-3-[4-(piperidin-1-yl)phenyl]acrylonitrile (**16**). According to procedure B, employment of 4-(piperidin-1-yl)benzaldehyde (492 mg, 2.60 mmol), benzyl cyanide (305 mg, 2.60 mmol), and pyrrolidine (185 mg, 2.60 mmol) gave rise to **16** as a yellow solid (150 mg, 0.52 mmol, 20%); mp 128 °C. <sup>1</sup>H NMR (CDCl<sub>3</sub>) δ 7.84 (psd, J = 8.9 Hz, 2H), 7.66–7.61 (m, 2H), 7.44–7.38 (m, 3H), 7.35–7.30 (m, 1H), 6.92 (psd, J = 7.8 Hz, 2H), 3.37–3.31 (m, 4H), 1.76–1.60 (m, 6H). <sup>13</sup>C NMR (CDCl<sub>3</sub>) δ 152.8, 142.4, 135.5, 131.4, 129.0, 128.3, 125.6, 123.2, 119.4, 114.5, 105.6, 48.9, 25.5, 24.5. HRMS (EI) calcd for C<sub>20</sub>H<sub>20</sub>N<sub>2</sub> [M]<sup>+</sup> 288.162649; found 288.164001. Anal. Calcd for C<sub>20</sub>H<sub>20</sub>N<sub>2</sub>: C, 83.30; H, 6.99; N, 9.71. Found: C, 83.23; H, 7.14; N, 9.81.

(Z)-3-[4-(Cyclohexylamino)phenyl]-2-phenylacrylonitrile (**18**). According to procedure C, utilization of (Z)-3-(4-bromophenyl)-2-phenylacrylonitrile (200 mg, 0.70 mmol), (±)-BINAP (32.9 mg, 0.053 mmol), Pd<sub>2</sub>(dba)<sub>3</sub> (32.2 mg, 0.035 mmol), sodium *tert*-butoxide (102 mg, 1.06 mmol), and cyclohexylamine (140 mg, 1.41 mmol) yielded, after purification by flash chromatography (*iso*-hexane/EtOAc, gradient from 0 to 25% in 12 min), **18** as a yellow solid (94 mg, 0.31 mmol, 44%); mp 122 °C. <sup>1</sup>H NMR (DMSO-*d*<sub>6</sub>) δ 7.74 (psd, J = 8.7 Hz, 2H), 7.69 (s, 1H), 7.64–7.60 (m, 2H), 7.45–7.39 (m, 2H), 7.33–7.28 (sm, 1H), 6.64 (psd, J = 8.7 Hz, 2H), 6.40 (d, J = 7.8 Hz, 1H), 3.33–3.23 (sm, 1H), 1.93–1.86 (sm, 2H), 1.74–1.65 (sm, 2H), 1.61–1.53 (sm, 1H), 1.39–1.27 (sm, 2H), 1.21–1.10 (m, 3H). <sup>13</sup>C NMR (CDCl<sub>3</sub>) δ 149.5, 142.8, 135.7, 131.7, 129.0, 128.1, 125.6, 122.3, 119.6, 112.6, 104.5, 51.4, 33.3, 25.8, 25.0. HRMS (EI) calcd for C<sub>21</sub>H<sub>22</sub>N<sub>2</sub> [M]<sup>+</sup> 302.178299; found 302.178004. Anal. Calcd for C<sub>21</sub>H<sub>22</sub>N<sub>2</sub>: C, 83.40; H, 7.33; N, 9.26. Found: C, 83.27; H, 7.26; N, 9.10.

(Z)-2-Phenyl-3-[4-(phenylamino)phenyl]acrylonitrile (**19**). Following procedure C, usage of (Z)-3-(4-bromophenyl)-2-phenylacrylonitrile (200 mg, 0.70 mmol), (±)-BINAP (32.9 mg, 0.053 mmol), Pd<sub>2</sub>(dba)<sub>3</sub> (32.2 mg, 0.035 mmol), sodium *tert*-butoxide (102 mg, 1.06 mmol), and aniline (131 mg, 1.41 mmol) yielded, after purification by flash chromatography (*iso*-hexane/EtOAc, gradient from 0 to 25% in 12 min), **19** as a yellow solid (110 mg, 0.37 mmol, 53%); mp 162 °C. <sup>1</sup>H NMR (CDCl<sub>3</sub>) δ 7.85 (psd, J = 8.7 Hz, 2H), 7.67–7.63 (m, 2H), 7.45–7.44 (m, 3H), 7.38–7.32 (m, 3H), 7.21–7.17 (m, 2H), 7.11–7.04 (m, 3H). <sup>13</sup>C NMR (CDCl<sub>3</sub>) δ 146.1, 142.1, 141.0, 135.2, 131.4, 129.6, 129.2, 128.6, 125.8, 125.5, 123.0, 120.2, 119.1, 115.7, 107.0. HRMS (EI) calcd for C<sub>21</sub>H<sub>16</sub>N<sub>2</sub> [M]<sup>+</sup> 296.131349; found 296.129489. Anal. Calcd for C<sub>21</sub>H<sub>16</sub>N<sub>2</sub>: C, 85.11; H, 5.44; N, 9.45. Found: C, 84.78; H, 5.66; N, 9.19.

(Z)-3-[4-(4-Methylpiperidin-1-yl)phenyl]-2-phenylacrylonitrile (**20**). According to procedure C, utilization of (Z)-3-(4-bromophenyl)-2-phenylacrylonitrile (200 mg, 0.70 mmol), (±)-BINAP (32.9 mg, 0.053 mmol), Pd<sub>2</sub>(dba)<sub>3</sub> (32.2 mg, 0.035 mmol), sodium *tert*-butoxide (102 mg, 1.06 mmol), and 4-methylpiperidine (140 mg, 1.41 mmol) rendered, after purification by flash chromatography (*iso*-hexane/DCM, 5:2), **20** as a yellow solid (194 mg, 0.64 mmol, 91%); mp 120 °C. <sup>1</sup>H NMR (DMSO-*d*<sub>6</sub>) δ 7.83 (psd, J = 8.9 Hz, 2H), 7.78 (s, 1H), 7.68–7.63 (m, 2H), 7.46–7.41 (m, 2H), 7.36–7.31 (sm, 1H), 6.99 (psd, J = 9.2 Hz, 2H), 3.92–3.85 (sm, 2H), 2.84–2.76 (sm, 2H), 1.69–1.62 (sm, 2H), 1.63–1.50 (sm, 1H), 1.21–1.08 (sm, 2H), 0.90 (d, J = 6.4 Hz, 3H). <sup>13</sup>C NMR (CDCl<sub>3</sub>) δ 152.6, 142.4, 135.5, 131.3, 129.0, 128.3, 125.6, 123.2, 119.4, 114.5, 105.6, 48.2, 33.7, 31.0, 22.0. HRMS (EI) calcd for C<sub>21</sub>H<sub>22</sub>N<sub>2</sub> [M]<sup>+</sup> 302.178299; found 302.178744. Anal. Calcd for C<sub>21</sub>H<sub>22</sub>N<sub>2</sub>: C, 83.40; H, 7.33; N, 9.26. Found: C, 83.20; H, 7.30; N, 8.81.

(Z)-2-Phenyl-3-[4-(piperazin-1-yl)phenyl]acrylonitrile (**22**). (Z)-3-(4-Bromophenyl)-2-phenylacrylonitrile (100 mg, 0.35 mmol) was dissolved in dry toluene (2 mL) under an argon atmosphere. Tri-*tert*-butylphosphine (14.2 mg, 0.070 mmol), Pd<sub>2</sub>(dba)<sub>3</sub> (16.1 mg, 0.018 mmol), sodium *tert*-butoxide (101 mg, 1.06 mmol), and piperazine (182 mg, 2.11 mmol) were added, and the suspension was stirred at 120 °C for 15 h. The reaction mixture was diluted with DCM, filtered through a pad of Celite, absorbed on silica gel, and purified by flash chromatography (DCM/methanol, 50:1), giving rise to **22** as a yellow wax (53.1 mg, 0.18 mmol, 52%). <sup>1</sup>H NMR (DMSO-*d*<sub>6</sub>) δ 7.84 (psd, J = 9.2 Hz, 2H), 7.80 (s, 1H), 7.68–7.64 (m, 2H), 7.47–7.41 (m, 2H),

7.37–7.31 (sm, 1H), 6.99 (psd, J = 9.2 Hz, 2H), 3.23–3.19 (sm, 4H), 2.81–2.77 (sm, 4H). <sup>13</sup>C NMR (CDCl<sub>3</sub>) δ 152.8, 142.2, 135.3, 131.2, 129.0, 128.4, 125.7, 124.1, 119.1, 114.5, 106.5, 48.8, 45.9. HRMS (EI) calcd for C<sub>19</sub>H<sub>19</sub>N<sub>3</sub> [M]<sup>+</sup> 289.157898; found 289.155945.

(Z)-3-[4-(4-Methylpiperazin-1-yl)phenyl]-2-phenylacrylonitrile (**23**). According to procedure B, employment of 4-(4-methylpiperazin-1-yl)benzaldehyde (265 mg, 1.30 mmol), benzyl cyanide (152 mg, 1.30 mmol), and pyrrolidine (92 mg, 1.30 mmol) furnished **23** as a yellow solid (268 mg, 0.88 mmol, 68%); mp 143 °C. <sup>1</sup>H NMR (DMSO-*d*<sub>6</sub>) δ 7.84 (psd, J = 8.9 Hz, 2H), 7.81 (s, 1H), 7.69–7.64 (m, 2H), 7.47–7.41 (m, 2H), 7.37–7.32 (sm, 1H), 7.02 (psd, J = 9.2 Hz, 2H), 3.30 (t, J = 5.0 Hz, 4H), 2.41 (t, J = 5.0 Hz, 4H), 2.19 (s, 3H). <sup>13</sup>C NMR (DMSO-*d*<sub>6</sub>) δ 152.7, 143.2, 135.2, 131.5, 129.6, 128.8, 125.7, 123.5, 119.5, 114.5, 104.7, 54.9, 47.2, 46.3. HRMS (EI) calcd for C<sub>20</sub>H<sub>21</sub>N<sub>3</sub> [M]<sup>+</sup> 303.173548; found 303.171852. Anal. Calcd for C<sub>20</sub>H<sub>21</sub>N<sub>3</sub>: C, 79.17; H, 6.98; N, 13.85. Found: C, 78.95; H, 7.01; N, 13.86.

(Z)-2-(4-Chlorophenyl)-3-[4-(dimethylamino)phenyl]acrylonitrile (**27**). According to procedure A, usage of 4-(dimethylamino)benzaldehyde (351 mg, 2.35 mmol), 2-(4-chlorophenyl)acetonitrile (357 mg, 2.35 mmol), and potassium hydroxide (132 mg, 2.35 mmol) furnished **27** as a yellow solid (326 mg, 1.15 mmol, 49%); mp 193 °C. <sup>1</sup>H NMR (CDCl<sub>3</sub>) δ 7.85 (psd, J = 8.9 Hz, 2H), 7.55 (psd, J = 8.9 Hz, 2H), 7.38–7.35 (m, 3H), 6.74 (psd, J = 8.9 Hz, 2H), 3.06 (s, 6H). <sup>13</sup>C NMR (CDCl<sub>3</sub>) δ 152.0, 142.9, 134.2, 133.8, 131.5, 129.1, 126.7, 121.4, 119.3, 111.7, 103.2, 40.2. HRMS (EI) calcd for C<sub>17</sub>H<sub>15</sub>ClN<sub>2</sub> [M]<sup>+</sup> 282.092376; found 282.093166. Anal. Calcd for C<sub>17</sub>H<sub>15</sub>ClN<sub>2</sub>: C, 72.21; H, 5.35; N, 9.91. Found: C, 72.06; H, 5.37; N, 9.85.

(Z)-2-(3-Chlorophenyl)-3-[4-(dimethylamino)phenyl]acrylonitrile (**28**). According to procedure A, employment of 4-(dimethylamino)benzaldehyde (585 mg, 3.92 mmol), 2-(3-chlorophenyl)acetonitrile (595 mg, 3.92 mmol), and potassium hydroxide (220 mg, 3.92 mmol) gave rise to **28** as a yellow solid (710 mg, 2.51 mmol, 49%); mp 132 °C. <sup>1</sup>H NMR (CDCl<sub>3</sub>) δ 7.85 (psd, J = 8.9 Hz, 2H), 7.60 (t, J = 1.9 Hz, 1H), 7.50 (sm, 1H), 7.38 (s, 1H), 7.33 (t, J = 7.8 Hz, 1H), 7.26 (sm, 1H), 6.71 (psd, J = 9.1 Hz, 2H), 3.06 (s, 6H). <sup>13</sup>C NMR (CDCl<sub>3</sub>) δ 152.0, 143.6, 137.6, 135.0, 131.7, 130.2, 127.9, 125.4, 123.7, 121.2, 119.2, 111.7, 102.8, 40.1. MS (EI) *m/z* (%) 282.1 (100) [M]<sup>+</sup>. Anal. Calcd for C<sub>17</sub>H<sub>15</sub>ClN<sub>2</sub>: C, 72.21; H, 5.35; N, 9.91. Found: C, 72.35; H, 5.51; N, 9.82.

(Z)-2-(2-Chlorophenyl)-3-[4-(dimethylamino)phenyl]acrylonitrile (**29**). Following procedure B, usage of 4-(dimethylamino)benzaldehyde (351 mg, 2.35 mmol), 2-(2-chlorophenyl)acetonitrile (357 mg, 2.35 mmol), and pyrrolidine (167 mg, 2.35 mmol) at 60 °C furnished **29** as a yellow solid (326 mg, 1.15 mmol, 49%); mp 99 °C. <sup>1</sup>H NMR (CDCl<sub>3</sub>) δ 7.85 (psd, J = 8.9 Hz, 2H), 7.46–7.40 (m, 2H), 7.33–7.26 (m, 2H), 7.12 (s, 1H), 6.73 (psd, J = 8.9 Hz, 2H), 3.06 (s, 6H). <sup>13</sup>C NMR (CDCl<sub>3</sub>) δ 152.0, 148.4, 135.6, 133.2, 131.5, 131.0, 130.4, 129.7, 127.4, 121.2, 119.0, 111.7, 101.8, 40.2. HRMS (EI) calcd for C<sub>17</sub>H<sub>15</sub>ClN<sub>2</sub> [M]<sup>+</sup> 282.092376; found 282.094431. Anal. Calcd for C<sub>17</sub>H<sub>15</sub>ClN<sub>2</sub>: C, 72.21; H, 5.35; N, 9.91. Found: C, 72.43; H, 5.53; N, 10.00.

(Z)-3-[4-(Dimethylamino)phenyl]-2-(2-iodophenyl)acrylonitrile (**30**). To a solution of 4-dimethylaminobenzaldehyde (161 mg, 1.08 mmol) and 2-(2-iodophenyl)acetonitrile (263 mg, 1.08 mmol) in methanol (2 mL) was added pyrrolidine (145 mg, 1.08 mmol), and the reaction mixture was stirred for 18 h at 60 °C. The reaction mixture was diluted with EtOAc, and the organic phase was washed with water, saturated potassium hydrogencarbonate solution, and brine, dried over MgSO<sub>4</sub>, filtered, and concentrated *in vacuo*. Flash chromatography (*iso*-hexane/EtOAc, gradient from 0 to 30% in 12 min) furnished **30** as a yellow solid (185 mg, 0.49 mmol, 46%); mp 134 °C. <sup>1</sup>H NMR (CDCl<sub>3</sub>) δ 7.94–7.91 (m, 1H), 7.85 (psd, J = 8.9 Hz, 2H), 7.42–7.36 (m, 2H), 7.04 (ddd, J = 7.7, 6.6, 2.5 Hz, 1H), 6.99 (s, 1H), 6.73 (psd, J = 9.2 Hz, 2H), 3.06 (s, 6H). <sup>13</sup>C NMR (CDCl<sub>3</sub>) δ 152.1, 148.5, 141.1, 140.1, 131.4, 130.5, 129.9, 128.7, 121.0, 118.8, 111.7, 106.6, 98.7, 40.2. HRMS (EI) calcd for C<sub>17</sub>H<sub>15</sub>IN<sub>2</sub> [M]<sup>+</sup> 374.028001; found 374.024834. Anal. Calcd for C<sub>17</sub>H<sub>15</sub>IN<sub>2</sub>: C, 54.56; H, 4.04; N, 7.49. Found: C, 54.82; H, 4.16; N, 7.45.

(Z)-2-(2-Bromophenyl)-3-[4-(dimethylamino)phenyl]acrylonitrile (**31**). A solution of 2-bromophenylacetonitrile (376 mg, 1.93 mmol)

and 4-dimethylaminobenzaldehyde (288 mg, 1.93 mmol) in morpholine (2 mL) was stirred for 12 h at 120 °C. The reaction mixture was absorbed onto silica, and flash chromatography (*iso*-hexane/EtOAc/DCM, 18:1:1) gave rise to **31** as yellow solid (184 mg, 0.56 mmol, 29%); mp 140 °C. <sup>1</sup>H NMR (CDCl<sub>3</sub>) δ 7.85 (psd, *J* = 8.9 Hz, 2H), 7.64 (dd, *J* = 8.0, 1.1 Hz, 1H), 7.41 (dd, *J* = 7.6, 1.8 Hz, 1H), 7.35 (td, *J* = 7.6, 1.4 Hz, 1H), 7.21 (ddd, *J* = 7.6, 1.8, 0.5 Hz, 1H), 7.07 (s, 1H), 6.72 (psd, *J* = 9.2 Hz, 2H), 3.06 (s, 6H). <sup>13</sup>C NMR (CDCl<sub>3</sub>) δ 152.1, 148.4, 137.5, 133.6, 131.4, 131.2, 129.8, 127.9, 123.2, 121.1, 118.9, 111.7, 103.5, 40.2. HRMS (EI) calcd for C<sub>17</sub>H<sub>15</sub>BrN<sub>2</sub> [M]<sup>+</sup> 326.041860; found 326.042488. Anal. Calcd for C<sub>17</sub>H<sub>15</sub>BrN<sub>2</sub>: C, 62.40; H, 4.62; N, 8.56. Found: C, 62.34; H, 4.79; N, 8.44.

(*Z*)-3-[4-(Dimethylamino)phenyl]-2-(2-methoxyphenyl)acrylonitrile (**32**). To a solution of 4-dimethylaminobenzaldehyde (304 mg, 2.04 mmol) and 2-(2-methoxyphenyl)acetonitrile (300 mg, 2.04 mmol) in methanol (4 mL) was added pyrrolidine (145 mg, 2.04 mmol), and the reaction mixture was stirred for 48 h at 60 °C. The reaction mixture was diluted with EtOAc, and the organic phase was washed with water, saturated potassium hydrogencarbonate solution, and brine, dried over MgSO<sub>4</sub>, filtered, and concentrated in vacuo. **32** was obtained after flash chromatography (cyclohexane/EtOAc/DCM, 8:1:1) as a yellow solid (111 mg, 0.40 mmol, 20%); mp 97 °C. <sup>1</sup>H NMR (CDCl<sub>3</sub>) δ 7.84 (psd, *J* = 8.7 Hz, 2H), 7.38 (dd, *J* = 7.6, 1.6 Hz, 1H), 7.32 (ddd, *J* = 8.2, 7.4, 1.6 Hz, 1H), 7.28 (s, 1H), 6.99 (td, *J* = 7.6, 1.1 Hz, 1H), 6.94 (dd, *J* = 8.2, 0.7 Hz, 1H), 6.76 (psd, *J* = 7.1 Hz, 2H), 3.91 (s, 3H), 3.05 (s, 6H). <sup>13</sup>C NMR (CDCl<sub>3</sub>) δ 157.0, 151.6, 146.5, 131.2, 129.9, 129.7, 125.9, 122.1, 121.0, 119.6, 111.6, 111.5, 102.0, 55.9, 40.2. HRMS (EI) calcd for C<sub>18</sub>H<sub>18</sub>N<sub>2</sub>O [M]<sup>+</sup> 278.141913; found 278.140550. Anal. Calcd for C<sub>18</sub>H<sub>18</sub>N<sub>2</sub>O: C, 77.67; H, 6.52; N, 10.06. Found: C, 77.25; H, 6.61; N, 9.74.

(*Z*)-3-[4-(Dimethylamino)phenyl]-2-(2-(trifluoromethyl)phenyl)acrylonitrile (**33**). A solution of 2-(2-(trifluoromethyl)phenyl)acetonitrile (200 mg, 1.08 mmol) and 4-dimethylaminobenzaldehyde (161 mg, 1.08 mmol) in morpholine (2 mL) was stirred for 24 h at 120 °C and subsequently absorbed onto silica gel. Flash chromatography (*iso*-hexane/EtOAc, 5:1) gave rise to **33** as a yellow solid (67 mg, 0.21 mmol, 20%); mp 110 °C. <sup>1</sup>H NMR (CDCl<sub>3</sub>) δ 7.82 (psd, *J* = 8.9 Hz, 2H), 7.76–7.72 (m, 1H), 7.61–7.56 (m, 1H), 7.52–7.46 (m, 2H), 6.98 (s, 1H), 6.80 (psd, *J* = 8.2 Hz, 2H), 3.07 (s, 6H). <sup>13</sup>C NMR (CDCl<sub>3</sub>) δ 152.1, 148.3, 147.1, 135.7, 132.2, 132.0, 131.3, 129.3, 128.7, 124.0 (d, *J*<sub>C,F</sub> = 274.0 Hz), 121.0, 119.2, 111.6, 100.7, 40.0. HRMS (EI) calcd for C<sub>18</sub>H<sub>15</sub>F<sub>3</sub>N<sub>2</sub> [M]<sup>+</sup> 316.118733; found 316.117731. Anal. Calcd for C<sub>18</sub>H<sub>15</sub>F<sub>3</sub>N<sub>2</sub>: C, 68.35; H, 4.78; N, 8.86. Found: C, 68.58; H, 5.18; N, 8.75.

(*Z*)-3-[4-(Dimethylamino)phenyl]-2-(2-fluorophenyl)acrylonitrile (**34**). Following procedure B, usage of 4-(dimethylamino)benzaldehyde (442 mg, 2.96 mmol), 2-(2-fluorophenyl)acetonitrile (400 mg, 2.96 mmol), and pyrrolidine (463 mg, 6.51 mmol) gave rise to **34** as a yellow solid (583 mg, 2.19 mmol, 74%); mp 106 °C. <sup>1</sup>H NMR (CDCl<sub>3</sub>) δ 7.86 (psd, *J* = 8.9 Hz, 2H), 7.54 (td, *J* = 7.8, 1.8 Hz, 1H), 7.42 (s, 1H), 7.32–7.26 (sm, 1H), 7.19 (td, *J* = 7.6, 1.1 Hz, 1H), 7.12 (ddd, *J* = 11.2, 8.2, 1.1 Hz, 1H), 6.71 (psd, *J* = 9.2 Hz, 2H), 3.06 (s, 6H). <sup>13</sup>C NMR (CDCl<sub>3</sub>) δ 159.8 (d, *J*<sub>C,F</sub> = 250.4 Hz), 152.0, 147.4 (d, *J*<sub>C,F</sub> = 7.8 Hz), 131.6, 129.7 (d, *J*<sub>C,F</sub> = 3.0 Hz), 129.6 (d, *J*<sub>C,F</sub> = 8.7 Hz), 124.6 (d, *J*<sub>C,F</sub> = 3.0 Hz), 124.2 (d, *J*<sub>C,F</sub> = 11.6 Hz), 121.5, 119.3, 116.5 (d, *J*<sub>C,F</sub> = 23.1 Hz), 111.6, 98.7 (d, *J*<sub>C,F</sub> = 1.9 Hz), 40.1. HRMS (EI) calcd for C<sub>17</sub>H<sub>15</sub>FN<sub>2</sub> [M]<sup>+</sup> 266.121927; found 266.123324. Anal. Calcd for C<sub>17</sub>H<sub>15</sub>FN<sub>2</sub>: C, 76.67; H, 5.68; N, 10.52. Found: C, 76.57; H, 5.73; N, 10.50.

(*Z*)-2-(2-Bromophenyl)-3-[4-(4-methylpiperazin-1-yl)phenyl]acrylonitrile Dihydrochloride (**37**). To a solution of 2-(2-bromophenyl)acetonitrile (480 mg, 2.45 mmol) and 4-(4-methylpiperazino)benzaldehyde (500 mg, 2.45 mmol) in methanol (4 mL) was added pyrrolidine (174 mg, 2.45 mmol). The reaction mixture was stirred for 48 h at 60 °C and subsequently absorbed onto silica gel. The free base was obtained by flash chromatography (DCM/MeOH, 49:1) and was afterward converted to the dihydrochloride salt **37** (806 mg, 1.93 mmol, 79% yield) by precipitation from EtOAc with HCl (5–6 M in *i*PrOH); mp above decomposition temperature. <sup>1</sup>H NMR (DMSO-*d*<sub>6</sub>, 80 °C, 500 MHz) δ 11.46 (bs, 1H), 9.96 (bs, 1H), 7.85 (psd, *J* = 8.9 Hz, 2H), 7.71 (d, *J* = 8.0 Hz, 1H), 7.51 (dd, *J* = 7.7, 1.7 Hz, 1H), 7.48–7.45 (sm, 1H),

7.37–7.33 (sm, 1H), 7.32 (s, 1H), 7.10 (psd, *J* = 8.9 Hz, 2H), 4.05–3.95 (m, 2H), 3.49–3.29 (m, 4H), 3.18–3.05 (m, 2H), 2.77 (s, 3H). <sup>13</sup>C NMR (DMSO-*d*<sub>6</sub>) δ 151.7, 148.6, 136.9, 133.7, 132.1, 131.4, 131.3, 129.1, 124.2, 122.8, 118.5, 115.3, 105.3, 52.1, 44.6, 42.4. HRMS (EI) calcd for C<sub>20</sub>H<sub>20</sub>BrN<sub>3</sub> [M]<sup>+</sup> 381.084059; found 381.087401. Anal. Calcd for C<sub>20</sub>H<sub>20</sub>BrCl<sub>2</sub>N<sub>3</sub>: C, 52.77; H, 4.87; N, 9.23. Found: C, 52.68; H, 4.97; N, 9.18.

**Time-Resolved Fluorescence Resonance Energy Transfer (TR-FRET) Assays in Vitro.** Ligand binding was determined by TR-FRET in vitro<sup>25</sup> using the Lanthascreen TR-FRET PPARβ/δ competitive binding assay as described.<sup>26,27</sup> The interaction of the PPARβ/δ LBD with a fluorescein-labeled corepressor peptide derived from the silencing mediator for retinoid and thyroid hormone receptors interaction domain 2 (SMRT-ID2) was determined using the Lanthascreen TR-FRET PPARβ/δ coregulator assay.<sup>27</sup> Assays were carried out and evaluated as described.

**Chemical Compound Library Screening.** The Open Chemical Repository of the NCI/NIH Developmental Therapeutics Program consisting of the Approved Oncology Drugs Set III (97 compounds), the Diversity Set III (1597 compounds), the Mechanistic Set (879 compounds), and the Natural Product Set II (120 compounds) was initially screened for compounds binding to the PPARβ/δ LBD using the competitive TR-FRET assay described above. Compounds showing significant competition (*n* = 129) were subsequently validated in triplicates using TR-FRET-based coactivator and corepressor peptide recruitment assays (see above).<sup>27</sup>

**Cell Culture.** WPMY-1 human myofibroblasts<sup>28</sup> (ATCC, CRL-2854), C2C12 murine myoblasts<sup>29</sup> (kindly provided by Dr. Thomas Braun, Bad Nauheim, Germany), and NIH3T3 cells were maintained in DMEM supplemented with 10% fetal bovine serum, 100 U/mL penicillin, and 100 μg/mL streptomycin in a humidified incubator at 37 °C and 5% CO<sub>2</sub>.

**Transcription, Gene Expression, and Chromatin Analyses.** Luciferase reporter assays were performed and evaluated as reported previously. LexA-PPAR expression plasmids and the 7-L-TATAi luciferase reporter construct have been described elsewhere.<sup>30,31</sup> RT-qPCR analyses of endogenous *Angptl4* expression and statistical analyses were carried out as described,<sup>17</sup> using *L27* as the normalizer. ChIP analysis was performed as reported elsewhere.<sup>24,32</sup>

**Pharmacokinetics in Mice.** In vivo pharmacokinetic studies were performed by Cerep, Redmond, WA. Briefly, compounds were formulated in DMSO/Solutol HS 15/PBS, pH 7.4 (5/5/90, v/v/v) and administered iv (1 mg/kg) and po (5 mg/kg) to male CD-1 mice by tail vein injection and gastric gavage, respectively. Blood samples were taken at eight time points post injection by parallel sampling (three mice each; see Figure 9 for details). Plasma samples were processed by acetonitrile precipitation and analyzed by HPLS-MS/MS following standard procedures.

## ■ ASSOCIATED CONTENT

### ● Supporting Information

Properties of compounds identified by library screening as PPARβ/δ ligands, Analysis of stilbene derivatives as potential PPARβ/δ ligands, Analysis of compound **1** (NSC636948) and derivatives by competitive in vitro ligand binding assay, and experimental procedures for further compounds. This material is available free of charge via the Internet at <http://pubs.acs.org>.

## ■ AUTHOR INFORMATION

### Corresponding Author

\*For W.D.: phone, +49 6421 2825810; E-mail, [wibke.diederich@staff.uni-marburg.de](mailto:wibke.diederich@staff.uni-marburg.de). For R.M.: phone, +49 6421 2866236; E-mail, [rmueller@imt.uni-marburg.de](mailto:rmueller@imt.uni-marburg.de).

### Author Contributions

§The first two authors contributed equally to this work.

### Notes

The authors declare no competing financial interest.

## ACKNOWLEDGMENTS

We thank Klaus Weber, Margitta Alt, and Julia Dick for expert technical assistance. This work is supported by grants to R.M. from the Deutsche Forschungsgemeinschaft (SFB-TR17/A3) and the LOEWE-Schwerpunkt "Tumor and Inflammation" of the state of Hesse.

## ABBREVIATIONS USED

ANGPTL4, angiopoietin-like 4 protein; *ANGPTL4*, angiopoietin-like 4 gene (human); *Angptl4*, angiopoietin-like 4 gene (mouse); BCL-6, B-cell chronic lymphatic leukemia/lymphoma 6 protein; CHIP, chromatin immune precipitation; CL, mean clearance; DBD, DNA binding domain; FRET, fluorescence resonance energy transfer; GST, glutathione S-transferase; HAT, acetyl transferase; HDAC, histone deacetylase; LBD, ligand binding domain; NCoR, nuclear receptor corepressor; *PDK4*, pyruvate dehydrogenase kinase 4 gene; PPAR, peroxisome proliferator-activated receptor; PPRE, peroxisome proliferator responsive element; RT-qPCR, real-time quantitative polymerase chain reaction; RXR, retinoid X receptor; SAR, structure-activity relationship; SMRT, silencing mediator for retinoid and thyroid hormone receptors; SMRT-ID2, SMRT interaction domain 2; SHARP, SMRT and HDAC-associated repressor protein; TR-FRET, time-resolved fluorescence resonance energy transfer; Vss, volume of distribution at steady state

## REFERENCES

- (1) Lonard, D. M.; O'Malley, B. W. Nuclear receptor coregulators: judges, juries, and executioners of cellular regulation. *Mol. Cell* **2007**, *27*, 691–700.
- (2) Desvergne, B.; Michalik, L.; Wahli, W. Transcriptional regulation of metabolism. *Physiol. Rev.* **2006**, *86*, 465–514.
- (3) Zoete, V.; Grosdidier, A.; Michielin, O. Peroxisome proliferator-activated receptor structures: ligand specificity, molecular switch and interactions with regulators. *Biochim. Biophys. Acta* **2007**, *1771*, 915–925.
- (4) Peraza, M. A.; Burdick, A. D.; Marin, H. E.; Gonzalez, F. J.; Peters, J. M. The toxicology of ligands for peroxisome proliferator-activated receptors (PPAR). *Toxicol. Sci.* **2006**, *90*, 269–295.
- (5) Glass, C. K.; Saijo, K. Nuclear receptor transrepression pathways that regulate inflammation in macrophages and T cells. *Nature Rev. Immunol.* **2010**, *10*, 365–376.
- (6) Michalik, L.; Wahli, W. Peroxisome proliferator-activated receptors (PPARs) in skin health, repair and disease. *Biochim. Biophys. Acta* **2007**, *1771*, 991–998.
- (7) Peters, J. M.; Gonzalez, F. J. Sorting out the functional role(s) of peroxisome proliferator-activated receptor-beta/delta (PPARbeta/delta) in cell proliferation and cancer. *Biochim. Biophys. Acta* **2009**, *1796*, 230–241.
- (8) Montagner, A.; Rando, G.; Degueurce, G.; Leuenberger, N.; Michalik, L.; Wahli, W. New insights into the role of PPARs. *Prostaglandins, Leukotrienes Essent. Fatty Acids* **2011**, *85*, 235–243.
- (9) Yu, S.; Reddy, J. K. Transcription coactivators for peroxisome proliferator-activated receptors. *Biochim. Biophys. Acta* **2007**, *1771*, 936–951.
- (10) Shi, Y.; Hon, M.; Evans, R. M. The peroxisome proliferator-activated receptor delta, an integrator of transcriptional repression and nuclear receptor signaling. *Proc. Natl. Acad. Sci. U.S.A.* **2002**, *99*, 2613–2618.
- (11) Adhikary, T.; Kaddatz, K.; Finkernagel, F.; Schönbauer, A.; Meissner, W.; Scharfe, M.; Jarek, M.; Blöcker, H.; Müller-Brüsselbach, S.; Müller, R. Genomewide analyses define different modes of transcriptional regulation by peroxisome proliferator-activated receptor-beta/delta (PPARbeta/delta). *PLoS One* **2011**, *6*, e16344.

- (12) Lee, C. H.; Chawla, A.; Urbiztondo, N.; Liao, D.; Boisvert, W. A.; Evans, R. M.; Curtiss, L. K. Transcriptional repression of atherogenic inflammation: modulation by PPARdelta. *Science* **2003**, *302*, 453–457.

- (13) Zaveri, N. T.; Sato, B. G.; Jiang, F.; Calaoagan, J.; Laderoute, K. R.; Murphy, B. J. A novel peroxisome proliferator-activated receptor delta antagonist, SR13904, has anti-proliferative activity in human cancer cells. *Cancer Biol. Ther.* **2009**, *8*, 1252–1261.

- (14) Shearer, B. G.; Wiethe, R. W.; Ashe, A.; Billin, A. N.; Way, J. M.; Stanley, T. B.; Wagner, C. D.; Xu, R. X.; Leesnitzer, L. M.; Merrihew, R. V.; Shearer, T. W.; Jeune, M. R.; Ulrich, J. C.; Willson, T. M. Identification and characterization of 4-chloro-N-(2-[[5-trifluoromethyl]-2-pyridyl]sulfonyl)ethyl)benzamide (GSK3787), a selective and irreversible peroxisome proliferator-activated receptor delta (PPARdelta) antagonist. *J. Med. Chem.* **2010**, *53*, 1857–1861.

- (15) Palkar, P. S.; Borland, M. G.; Naruhn, S.; Ferry, C. H.; Lee, C.; Sk, U. H.; Sharma, A. K.; Amin, S.; Murray, I. A.; Anderson, C. R.; Perdew, G. H.; Gonzalez, F. J.; Müller, R.; Peters, J. M. Cellular and pharmacological selectivity of the peroxisome proliferator-activated receptor-beta/delta antagonist GSK3787. *Mol. Pharmacol.* **2010**, *78*, 419–430.

- (16) Shearer, B. G.; Steger, D. J.; Way, J. M.; Stanley, T. B.; Lobe, D. C.; Grillot, D. A.; Iannone, M. A.; Lazar, M. A.; Willson, T. M.; Billin, A. N. Identification and characterization of a selective peroxisome proliferator-activated receptor beta/delta (NR1C2) antagonist. *Mol. Endocrinol.* **2008**, *22*, 523–529.

- (17) Naruhn, S.; Toth, P. M.; Adhikary, T.; Kaddatz, K.; Pape, V.; Dörr, S.; Klebe, G.; Müller-Brüsselbach, S.; Diederich, W. E.; Müller, R. High-affinity peroxisome proliferator-activated receptor beta/delta-specific ligands with pure antagonistic or inverse agonistic properties. *Mol. Pharmacol.* **2011**, *80*, 828–838.

- (18) Toth, P. M.; Naruhn, S.; Pape, V. F.; Dörr, S. M.; Klebe, G.; Müller, R.; Diederich, W. E. Development of Improved PPARbeta/delta Inhibitors. *ChemMedChem* **2012**, *7*, 159–170.

- (19) Kasuga, J.; Ishida, S.; Yamasaki, D.; Makishima, M.; Doi, T.; Hashimoto, Y.; Miyachi, H. Novel biphenylcarboxylic acid peroxisome proliferator-activated receptor (PPAR) delta selective antagonists. *Bioorg. Med. Chem. Lett.* **2009**, *19*, 6595–6599.

- (20) Guram, A. S.; Rennels, R. A.; Buchwald, S. L. A Simple Catalytic Method for the Conversion of Aryl Bromides to Arylamines. *Angew. Chem., Int. Ed.* **1995**, *34*, 1348–1350.

- (21) Jiang, L.; Buchwald, S. L. *Palladium-Catalyzed Aromatic Carbon-Nitrogen Bond Formation*; WILEY-VCH Verlag GmbH & Co: Weinheim, Germany, 2004; Vol. 2, pp 699–760.

- (22) Louie, J.; Hartwig, J. F. Palladium-catalyzed synthesis of arylamines from aryl halides. Mechanistic studies lead to coupling in the absence of tin reagents. *Tetrahedron Lett.* **1995**, *36*, 3609–3612.

- (23) Mandard, S.; Zandbergen, F.; Tan, N. S.; Escher, P.; Patsouris, D.; Koenig, W.; Kleemann, R.; Bakker, A.; Veenman, F.; Wahli, W.; Müller, M.; Kersten, S. The direct peroxisome proliferator-activated receptor target fasting-induced adipose factor (FIAF/PGAR/ANGPTL4) is present in blood plasma as a truncated protein that is increased by fenofibrate treatment. *J. Biol. Chem.* **2004**, *279*, 34411–34420.

- (24) Kaddatz, K.; Adhikary, T.; Finkernagel, F.; Meissner, W.; Müller-Brüsselbach, S.; Müller, R. Transcriptional profiling identifies functional interactions of TGFβ and PPARβ/δ signaling: synergistic induction of ANGPTL4 transcription. *J. Biol. Chem.* **2010**, *285*, 29469–29479.

- (25) Staflieni, D. K.; Vedvik, K. L.; De Rosier, T.; Ozers, M. S. Analysis of ligand-dependent recruitment of coactivator peptides to RXRbeta in a time-resolved fluorescence resonance energy transfer assay. *Mol. Cell. Endocrinol.* **2007**, *264*, 82–89.

- (26) Rieck, M.; Meissner, W.; Ries, S.; Müller-Brüsselbach, S.; Müller, R. Ligand-mediated regulation of peroxisome proliferator-activated receptor (PPAR) beta/delta: a comparative analysis of PPAR-selective agonists and all-trans retinoic acid. *Mol. Pharmacol.* **2008**, *74*, 1269–1277.

- (27) Naruhn, S.; Meissner, W.; Adhikary, T.; Kaddatz, K.; Klein, T.; Watzel, B.; Müller-Brüsselbach, S.; Müller, R. 15-Hydroxyeicosatetraenoic

acid is a preferential peroxisome proliferator-activated receptor  $\beta/\delta$  agonist. *Mol. Pharmacol.* **2010**, *77*, 171–184.

(28) Webber, M. M.; Trakul, N.; Thraves, P. S.; Bello-DeOcampo, D.; Chu, W. W.; Storto, P. D.; Huard, T. K.; Rhim, J. S.; Williams, D. E. A human prostatic stromal myofibroblast cell line WPMY-1: a model for stromal–epithelial interactions in prostatic neoplasia. *Carcinogenesis* **1999**, *20*, 1185–1192.

(29) Yaffe, D.; Saxel, O. Serial passaging and differentiation of myogenic cells isolated from dystrophic mouse muscle. *Nature* **1977**, *270*, 725–727.

(30) Fauti, T.; Müller-Brüsselbach, S.; Kreutzer, M.; Rieck, M.; Meissner, W.; Rapp, U.; Schweer, H.; Kömhoff, M.; Müller, R. Induction of PPARbeta and prostacyclin (PGI<sub>2</sub>) synthesis by Raf signaling: failure of PGI<sub>2</sub> to activate PPARbeta. *FEBS J.* **2006**, *273*, 170–179.

(31) Jérôme, V.; Müller, R. Tissue-specific, cell cycle-regulated chimeric transcription factors for the targeting of gene expression to tumor cells. *Hum. Gene Ther.* **1998**, *9*, 2653–2659.

(32) Stockert, J.; Adhikary, T.; Kaddatz, K.; Finkernagel, F.; Meissner, W.; Müller-Brüsselbach, S.; Müller, R. Reverse crosstalk of TGF $\beta$  and PPAR $\beta/\delta$  signaling identified by transcriptional profiling. *Nucleic Acids Res.* **2011**, *39*, 119–131.